

WFPC2 Pointing Uncertainties

Gabriel Brammer, Brad Whitmore, and Anton Koekemoer

Space Telescope Science Institute, 3700 San Martin Drive, Baltimore, MD 21218

Abstract. This paper examines the absolute pointing of WFPC2 using repeat observations of GRW+70D5824, our photometric monitoring star. An offset of 1–2'' is found between the intended pointing position—pixel (420,424.5) on the PC (PC1)—and the observed pointing positions. This offset manifests itself as a circular annulus of data points centered around PC1 due to changing roll angles of *HST* during the year, which hence increases the observed pointing scatter from the expected $\sim 1''$ (due to uncertainties in the guide stars) to 2–3''. This issue is not critical for most WFPC2 users since the camera has a large field of view. Users requiring better absolute astrometric precision should measure positions relative to astrometric standards on the same image frame, if they exist.

1. Introduction

The absolute pointing of WFPC2, with its wide field of view, is not as critically important as it is for some of the other *HST* science instruments that require placing a target on apertures as small as a 5'' square, (e.g., STIS). However, occasionally such accuracy is desired for specific target placement on the WFPC2 chips. The absolute pointing of WFPC2 has not been extensively studied in the past, and a more careful characterization of the absolute pointing could be useful for estimating the reliability of both past and future WFPC2 pointings.

Following Servicing Mission 3B, a jump was noticed in the relative alignments between the three Fine Guidance Sensors of the FGS. The team monitoring the FGS alignment wanted to see if this jump was visible in WFPC2 observations, motivating the accumulation of the dataset described here.

2. Dataset

The observations used here to monitor the pointing of WFPC2 come from observations of the WFPC2 standard star GRW+70D5824 taken for the monthly photometric monitor program (Gonzaga et al. 2003). The star has been consistently observed since 1994 in 9 filters on both the PC and WF3 chips, with less frequent observations on the other two WF chips. The sample analyzed here contains 92 observations beginning Jan 2, 1999, through Aug 11, 2002, using the PC and filter F555W.

These data provide an opportunity to monitor the absolute pointing of WFPC2, as the star would ideally be consistently placed at the same pixel location on the chip with some associated scatter due to uncertainties in the guide star positions ($\sim 1''$). The expected pixel position here corresponds to the PC1 aperture located at (420,424.5) on the PC. The observed positions of GRW+70D5824 are shown in Figure 1.

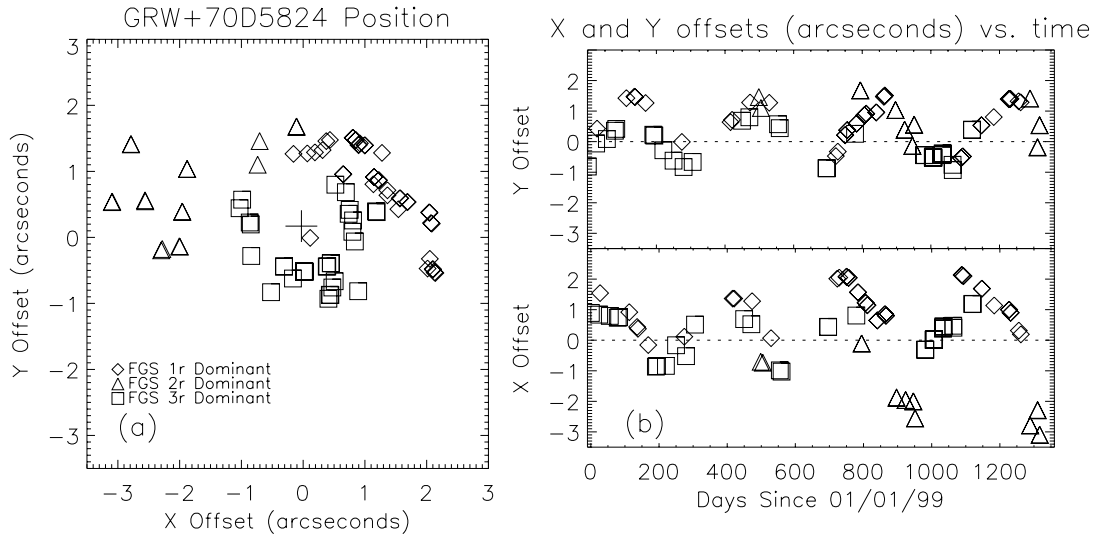


Figure 1. (a) GRW+70D5824 positions on the PC from Jan 1999 to Aug 2002. The different point styles indicate which Fine Guidance Sensor was dominant for the particular observation. The offsets are relative to the PC1 aperture position, marked by “+”. The plate scale of the PC is $\sim 0.05''/\text{pixel}$. (b) x and y GRW+70D5824 positions vs. time. The sinusoidal oscillations in each direction have a period of ~ 365 days.

3. Analysis

The standard star pointings plotted in Figure 1a do not scatter randomly around PC1. Rather, they are distributed in an approximately circular annulus centered around the PC1 aperture location. If the points of Figure 1a are plotted consecutively in time, then the star’s location on the chip appears to rotate in the counterclockwise direction about PC1. This rotation is manifested in the out-of-phase sinusoidal variations of x and y position with time, shown in Figure 1b.

Such a rotation is caused by a pointing offset in RA and/or declination whose projection on the camera x and y axes changes as the orientation of the telescope rotates. The orientation angle rotates through 360° over the course of the year. To estimate the WFPC2 pointing uncertainty without the effect of the pointing offset, we modeled the rotation of the data points by “de-rotating” them by an angle ϕ , relative to an arbitrary reference observation. The angle ϕ (in radians) used is then:

$$\phi = \frac{(MJD - MJD_{\text{ref}})}{365} \times 2\pi.$$

The “de-rotated” result is shown in Figure 2a, with $MJD_{\text{ref}} = 51371$ (Jul 12, 1999).

Another model fitting a sinusoidal function to the points of Figure 1b for each guidance sensor individually and plotting the residuals was used to compare with the rotation model. The amplitude and vertical offset were fit for each FGS in both x and y , while the phase and period were set to the values that produced the best fit in FGS3. For each FGS, the fitted vertical offset was added to the residuals to predict the offset caused by the misalignment. The fit residuals are shown in Figure 2c for comparison with the results of the “de-rotation” model. A comparison of the rms scatter of the points for each FGS before and after applying both models is shown in Table 1.

Table 1. Rms before and after De-rotating (in arcseconds)

Dominant FGS	initial	“de-rotated”	“sine-fit”	initial	“de-rotated”	“sine-fit”
	(x)	(x)	(x)	(y)	(y)	(y)
FGS1r	0.65	0.61	0.28	0.66	0.56	0.25
FGS2r	0.91	0.41	0.47	0.63	0.90	0.44
FGS3	0.62	0.21	0.18	0.51	0.29	0.21

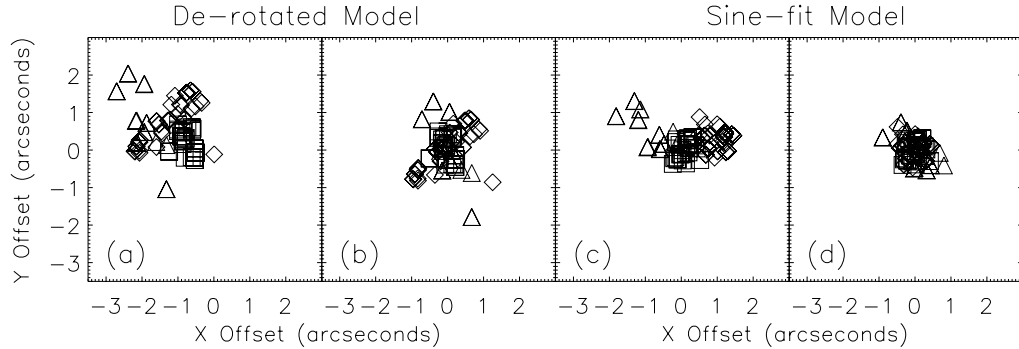


Figure 2. **(a)** “De-rotated” pointing positions. The positions fall into distinct groups according to which FGS was dominant for a particular pointing. The “ θ ” position of the groups about the origin depends on the choice of the arbitrary reference observation, so this model does not indicate the physical direction of the misalignment offsets for each FGS. **(b)** Predicted distribution of pointings after the aperture update implemented Oct 20, 2002, to correct the FGS-FGS misalignments. This plot centers the mean position of the pointings for each FGS on (0,0). **(c,d)** Same as **a,b** for the residuals of the sine-fit model. Note how the points are more tightly distributed, and how they continue to fall into discrete groups according to dominant FGS.

4. Conclusions

The most obvious feature of the plots before and after modeling the rotation of the data points is that the pointing locations clearly fall into discrete regions according to which Fine Guidance Sensor was dominant for a given pointing. This indicates a relative misalignment between the guidance sensors, which has been previously seen in FGS monitors using STIS.

The pointings using FGS3 as dominant show the smallest rms after removing the rotation effect, shown in Figures 2a,c and lie closest to the expected pointing of the PC1 aperture location. The rms scatter of these pointings decreases by a factor of about 2.5 in both x and y after compensating for the rotation. Where FGS 1r was dominant, the pointings show a smaller decrease in scatter after removing the rotation, and there is minimal improvement seen for pointings using FGS 2r. Both the scatter in the pointings, and the amount by which the pointings miss the aperture position, are largest for pointings in which FGS 2r was dominant.

These results confirm STIS monitors that indicate that pointings using FGS 3 are the most accurate and precise of the three, while FGS 2r pointings show significant scatter and experience more frequent pointing failures. These results can be used as a “before” picture of the WFPC2 pointings to compare with results of pointings made after the observatory

aperture file was updated on Oct 20, 2002 to correct for the misaligned guidance sensors. After the aperture correction, we would expect all of the pointings in all three guidance sensors to be distributed randomly about PC1, or the desired pointing position, with a small rms scatter caused by the astrometric accuracy limits of the guide star catalogs. To estimate the improvement in pointing precision after the update, we shifted the pointing position for each FGS to a common mean and plot the results in Figure 2b,d. Combining this shift and the rotation from above, the rms scatter of all of the pointings decreases by 70–80% in x and 10–40% in y . Since the orientations of x and y are arbitrary in the model, the characteristic rms after the aperture update should show a decrease of 50–70% after Oct 20, 2002. We will determine the actual updated WFPC2 pointing statistics from subsequent GRW+70D5824 observations taken over the coming months.

Table 2. Rms before and after De-rotating (in arcseconds)

Dominant FGS	initial (x)	“de-rotated” (x)	“sine-fit” (x)	initial (y)	“de-rotated” (y)	“sine-fit” (y)
FGS1r	0.65	0.61	0.28	0.66	0.56	0.25
FGS2r	0.91	0.41	0.47	0.63	0.90	0.44
FGS3	0.62	0.21	0.18	0.51	0.29	0.21

Acknowledgments. We would like to thank Olivia Lupie and Colin Cox for their FGS expertise.

References

Gonzaga, S., Ritchie, C., Baggett, S., Whitmore, B., Casertano, S. 2003, *Technical Instrument Report WFPC2* (Baltimore: STScI), to be released in early 2003